

Effects of Propellant and Electrode Geometry on Pulsed Ablative Plasma Thruster Performance

D.J. Palumbo* and W.J. Guman†

Fairchild Industries, Fairchild Republic Co., Farmingdale, N. Y.

A performance level compatible with 30% thrust efficiency at 1500 s specific impulse at 1 mlb (4.45 mN) of thrust was demonstrated with the parallel rail pulsed ablative thruster using Teflon propellant. Parametric variations of interelectrode spacing and included angle were performed. In addition, Teflon was replaced by other thermoplastics and was also seeded with 10% and 30% LiOH and InBr in an evaluation of alternative propellants. Both the conventional breech-fed and later side-feed electrode/propellant configurations were tested. With the same initial conditions it was shown that the breech-fed geometry yields higher thrust efficiency than the side-feed geometry because of the higher specific impulse generated (i.e., up to 5300 s using Teflon). Results of parametric studies indicate that, for high thrust/power and moderately high specific impulse, virgin Teflon propellant with an interelectrode spacing of 3.0 in. (7.62 cm) and zero degree interelectrode included angle in the side-fed configuration are best. A simple semiempirical analytic model is presented where it is shown that the broad range in performance characteristic of this device is related to the degree to which magnetoplasmadynamic and ordinary gasdynamic acceleration mechanisms can be made more or less dominant in the acceleration of the ablated propellant.

Introduction

EARLY development of solid propellant pulsed ablative thrusters using Teflon propellant produced micropound thrust devices. In 1968, four of these thrusters were flown on Lincoln Experimental Satellite 6 (LES-6) and were highly successful.¹ Upcoming flight-qualified hardware was developed for three-axis attitude control on LES-9,² and for drag compensation on TIP-2. The inherent operational simplicity of this electric propulsive device has inspired programs to increase performance and broaden its applicability. The original microthruster has been successively scaled up from the 6 μ lb-s (26.67 μ N-s) impulse bit delivered by the LES-6 thruster to a current capability of 6 mlb-s (26.67 mN-s). Thrust efficiency has also been improved. Latest laboratory testing has resulted in thrust efficiencies as high as 53% at 5300 s specific impulse.³

Original microthrusters utilized the breech-fed parallel rail electrode/propellant configuration with planar ablation surface (Fig. 1). Improvement in the thrust/power T/P ratio was later realized when the V-shaped ablation surface depicted in Fig. 2 was investigated, and eventually this evolved into the side-fed geometry with parallel planar ablation surfaces shown in Fig. 3. This article is a summary of the data obtained by varying the interelectrode spacing H and electrode included angle ϕ . Also reported on are the results of other propellants and a simple analysis to determine the salient parameters relating to thruster efficiency.

Test Thruster and Instrumentation

To carry out performance evaluations, a thruster was constructed utilizing up to 12 oil-impregnated Mylar capacitors, each having a capacitance of 9 μ f. The capacitors were assembled into a self-supporting low inductance discharge circuit by mounting them along radial lines equidistant from the center of a 22-in. (55.9-cm) diameter negative collector plate and 18-

in. (45.7-cm) diameter positive collector plate separated by two sheets of 5-mil (0.13-mm) Mylar for insulation. Strip lines, fastened to the center of these plates, carry the current to the electrode assembly. All current carrying elements are copper and all interfaces are bolted. Inductive shock excitation of this assembly shorted with a length of 0.041-in.

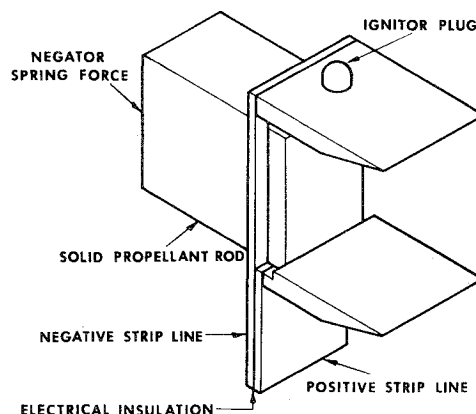


Fig. 1 Breech-fed electrode/propellant geometry with planar ablation surface.

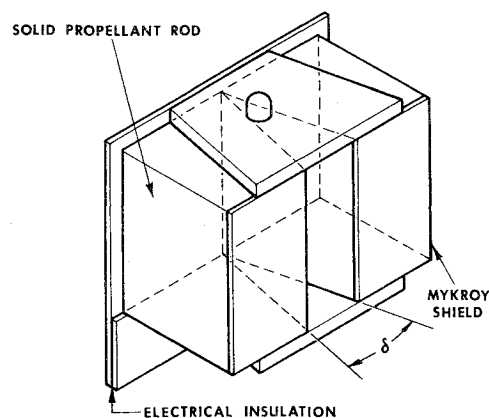


Fig. 2 Breech-fed electrode/propellant geometry with V-shaped ablation surface.

Presented as Paper 75-409 at the AIAA 11th Electric Propulsion Conference, New Orleans Louisiana, March 19-21, 1975; submitted March 19, 1975; revision received September 24, 1975. This research was performed for the Air Force Rocket Propulsion Laboratory under Contract F04611-72-C-0053.

Index categories: Electric and Advanced Space Propulsion; Material Ablation; Fuels and Propellants, Properties of.

*Research Engineer, Plasma Propulsion Group, Associate AIAA.

†Chief of Electric Propulsion, Associate Fellow AIAA.

(1-mm) copper wire between the cathode and anode yielded an inductance of 60 nH and resistance of 2.6 mΩ for the assembly, when corrected for the inductance of the shorting wire. Techniques used to measure thruster performance and other parameters cited in this article are described in detail in Ref. 3.

Results of Parametric Studies

Effect of Included Angle between Electrodes

A series of thruster performance tests were run at 450 J discharge energy to assess the effect of the included angle between electrodes (ϕ in Fig. 3) on thruster performance. The interelectrode spacing H and propellant rod spacing W were held constant at 7.62 cm and 9.53 mm, respectively, during these tests. The electrode length was 4.06 cm and the width 3.81 cm in all cases.

The configurations considered were the side-feed and breech geometries. The propellant length d in the side-feed geometry was 3.35 cm. In the breech-fed case the propellant was a 6.35-mm thick slab of Teflon measuring 1.9 cm wide and 7.42 cm high.

Results are presented graphically in Fig. 4. It was observed that a significant increase in performance level was realized for both geometries by increasing the electrode angle from zero to 20 deg. In particular, the thrust/power ratio of the breech geometry was increased from 20.4 mN/kW to 21.1 mN/kW, while specific impulse also increased from 4730 s to 5160 s. Increases in both of these parameters resulted in a 6.1% increase in efficiency (from 47.3% to 53.4%). A similar trend was observed for the side-feed geometry. Although the thrust/power increment was within the range of experimental accuracy, the specific impulse showed a 24.3% increase from 1030 s to 1280. Efficiency was, therefore, increased from 18.9% to 23.6%.

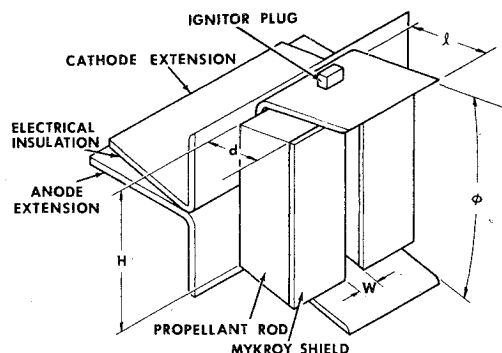


Fig. 3 Side-fed electrode/propellant geometry with parallel ablation surfaces.

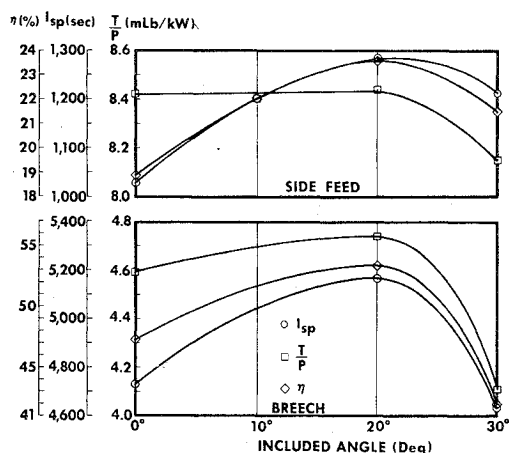


Fig. 4 Thruster performance of side-fed and breech-fed planar configurations as function of electrode included angle at an interelectrode spacing of 7.62 cm.

A further increase in the electrode angle to 30 deg led to a considerable decrease in performance for both propellant configurations. Thrust/power ratio and specific impulse dropped significantly. In an attempt to refine the electrode geometry further, one additional test was performed at a 10-deg electrode included angle. This test was performed on the side-feed geometry. The performance level fell between that measured at the 0 and 20-deg angles. A test at the 10 deg angle was not performed on the breech geometry.

This series of parametric tests revealed an optimum electrode angle for thruster efficiency at the 450-joule energy level. The thrust/power ratio, however, is relatively insensitive to the included electrode angle in the side-feed configuration at angles less than the optimum, and falls off rapidly at angles greater than optimum.

Effect of Interelectrode Spacing

Performance testing to appraise the effects of interelectrode spacing H were carried out using the 20 deg included electrode angle. All other parameters were held constant, except the propellant length d . To obtain a meaningful comparison of results it was necessary to change d with H so as to retain approximately the same propellant area exposed to the discharge. This was done because it is known that an increase in the discharge energy to exposed propellant area ratio (E_0/A_p) will automatically lead to an increase in specific impulse, all other factors being the same.⁴ The results of this series of experiments are presented in Fig. 5.

Interelectrode spacings of 6.6, 7.62, and 10.16 cm were tested with corresponding ratios of E_0/A_p equal to 8.56, 9.59, and 8.80 J/sq cm. The data indicate a monotonic trend toward lower thrust/power and higher specific impulse as the interelectrode spacing is increased. Efficiency, however, is highest at the 7.62-cm spacing and falls off rapidly from 23.6% to 19.2% while the thrust/power ratio T/P increases from 37.52 mN/kW to 38.76 mN/kW when H is decreased to 6.60 cm. The increase in T/P afforded by decreasing H is, therefore, accompanied by a much stronger drop in specific impulse. It was also observed, by monitoring the response of a Rogowski coil which measured total discharge current, that as H decreased the discharge became more oscillatory, and that even though E_0/A_p was approximately the same in all tests, a larger amount of mass per discharge was obtained as H was decreased.

Additional experimentation at the 10.16-cm spacing included two tests in which the propellant area was increased. These tests were performed to explore further the effect of introducing additional mass into the discharge, all other parameters remaining constant. In the first test the propellant area was increased from 53.4 sq cm to 66.7 sq cm. This resulted in an increase in mass per discharge from 0.849 to 1.158 mg, accompanied by an increase in T/P from 28.67 to 33.03 mN/kW and decreases in I_{sp} and η to 1060 s at 18.2%. Further increasing the propellant area to 77.42 sq cm increased the mass per discharge to 1.54 mg and thrust/power

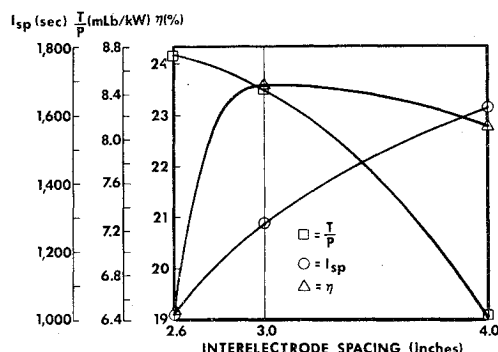


Fig. 5 Thruster performance of side-fed configuration as function of interelectrode spacing with an electrode included angle of 20°.

Table 1 Results of performance tests on different plastics

Propellant	Teflon	Celcon	Halar	Tefzel	Halon
E_0 (J)	454	436	-	416	381
T/P (mN/kW)	21.07	17.91	-	16.05	17.47
I_{sp} (s)	5170	5500	-	8410	5100
η (%)	53.4	48.3	Charred	66.2	48.7

ratio to 34.85 mN/kW with decreases in I_{sp} and η to 1060 s at 18.2%. These tests further suggest that the introduction of more propellant mass, all other parameters held constant, reduces the efficiency of this device at a given discharge energy.

Results of Propellant Studies

Evaluation of Alternate Thermoplastics

Four different thermoplastics other than Teflon were evaluated as possible alternative propellants. These were Celcon, Halar, Tefzel, and unsintered Halon.

Results of performance testing with these thermoplastics are presented in Table 1. None of the alternate plastics produce a thrust/power ratio comparable to Teflon and, with the exception of Tefzel, specific impulse are in the same neighborhood as that of Teflon. Halar was char forming, which resulted in a noticeable decrease in impulse bit amplitude as a function of operating time during the performance test. The surface of this plastic exposed to the discharge was completely black after approximately 1000 discharges. The replacement of the two fluorine atoms by two hydrogen atoms in Tefzel, as opposed to Teflon, is probably the reason for the high specific impulse measured since the molecular weight of the resulting plasma is conceivably lower. The presence of hydrogen in Celcon is probably offset by the addition of an oxygen atom.

Evaluation of Seeded Teflon Propellants

Teflon was seeded prior to sintering with 10% and 30% LiOH and InBr. It was not possible to obtain an overall performance evaluation for the LiOH seeded samples because a significant monotonic decrease in the impulse bit was observed during testing of both samples. This is shown in Fig. 6, where impulse bit as a function of number of discharges is plotted for both mixtures. Typical data using pure Teflon are also presented for reference. Changes in the current waveform were also observed during the tests. In particular, peak current decreased as the number of discharges increased. This led to the supposition that a high-resistance compound was precipitating out on the electrodes. To test this hypothesis, the electrodes were cleaned after 1000 discharges and replaced. Resumption of testing revealed that the impulse bit had recovered to its initial value. This was proof that, indeed, some low-conductivity deposit had settled out on the electrodes with each discharge, thereby increasing resistive losses and allowing less energy to enter the plasma.

Tests on the InBr seeded samples proceeded with no noticeable abnormalities. A summary of the data obtained

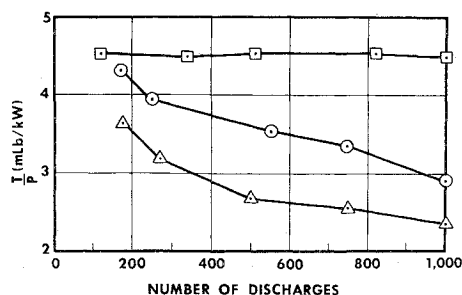


Fig. 6 Thrust power ratio as function of number of discharges for □-Teflon, ○-10% LiOH/90% Teflon, and △-30% LiOH/70% Teflon.

Table 2 Results of performance tests on InBr/Teflon propellants

Propellant	100% TFE	10% InBr/90% TFE	30% InBr/70% TFE
E_0 (J)	390	387	400
T/P (mN/kW)	20.14	20.45	19.47
I_{sp} (s)	4610	4500	4901
η (%)	45.4	45.1	38.3

using the InBr seeded samples as well as a test in which pure Teflon was used is presented in Table 2. As evidenced by the data, no significant increase in performance was realized by seeding Teflon with InBr in the percentages indicated.

Thrust Efficiency in Pulsed Ablative Plasma Accelerators

Pulsed ablative plasma acceleration is unique in that the acceleration process is completely unsteady and includes both electrothermal and electromagnetic energy transfer from the storage capacitor to the plasma.

Electrothermal transfer of energy to the plasma is a result of its finite electrical conductivity, leading to resistive heating. Because the acceleration process is basically an unsteady expansion, a part of the added heat is converted to useful kinetic energy.

Charged particle acceleration may also occur due to thermal expansion of the plasma. A more significant mechanism for their acceleration, however, is due to the presence of a self-induced magnetic field, produced by current flowing from the storage capacitor through the plasma. Since the current and magnetic flux lines cross each other, a net Lorentz force is experienced by the charged particles. In a continuum analysis, this force has the same effect on momentum flux as an ordinary thermodynamic pressure.

To generate some insight into what parameters affect thrust efficiency, a simple analysis was performed in which the two mechanisms cited are considered to be independent of one another and their contributions to the impulse bit are determined. Ordinary gasdynamic expansion of a gas having mass M_1 and energy E_1 into a vacuum from a duct of constant cross-sectional area has been treated in detail by Stanyukovich.⁵ The impulse produced by such a process is denoted I_{OGD} (ordinary gasdynamic) and is given by

$$I_{OGD} = \xi (2M_1 E_1)^{1/2} \quad (1)$$

where ξ is a function of the ratio of specific heats γ , which varies from 0.796 for $\gamma=1$ to 0.865 for $\gamma=3$.

The electromagnetic contribution to the impulse bit is assumed to be the result of the time integral of magnetic pressure forces against the back wall of the nozzle. If variations in magnetic flux density in the two lateral directions of the nozzle are assumed negligible, the instantaneous force is simply given by

$$F(t) = 0.5 H W B_{wall}^2 / \mu \quad (2)$$

where μ is the permeability of the plasma and B_{wall} is the flux density.

Under the above conditions Faraday's law leads to

$$B_{wall} = \mu i(t) / W \quad (3)$$

where $i(t)$ is the instantaneous discharge current.

The validity of Eq. (3) was demonstrated during another program.⁶ Substitution of Eq. (3) into Eq. (2) and integration in time over the discharge period gives the impulse due to electromagnetic forces, denoted I_{EM}

$$I_{EM} = (\mu H/2W) \int_0^\infty i^2 dt \quad (4)$$

Summation of Eqs. (1) and (4) gives the total impulse bit. In general, M_I and E_I will be fractions of the total mass ablated during the discharge m and the total energy initially stored in the capacitor E . Combining these fractions and the parameter ξ into a single constant K_I and letting $K_2 = \mu H/2W$ one obtains

$$I = K_I (2mE)^{1/2} + K_2 \Psi \quad (5)$$

where Ψ denotes the integral of current squared over time.

The definition of thrust efficiency leads to the following expression for pulsed devices:

$$\eta_T = I^2 / (2mE) \quad (6)$$

Dividing Eq. (5) by $(2mE)^{1/2}$ yields

$$\eta_I = \eta_T^{1/2} = K_I + K_2 \Psi / (2mE)^{1/2} = K_I + K_2 \lambda \quad (7)$$

where η_I is defined as the square root of thrust efficiency.⁷ The values of Ψ , m , E and η_T obtained from performance testing were used to check for a correlation of η_I with λ . The results are plotted in Fig. 7. An excellent correlation between these parameters does exist for each of the interelectrode spacings tested. Moreover, since K_2 should be proportional to H , replotting these data using $H\lambda$ as the abscissa reduces the difference in slope between the three straight lines from 0.54, 0.80, and 1.23 at $H=6.60$, 7.62, and 10.16 cm, respectively, to 0.8, 0.10, and 0.12. The data then fall on a single line, within the experimental error.

The trend towards increased efficiency with Ψ indicates that to generate higher efficiencies the electromagnetic processes must be amplified over the ordinary gasdynamic expansion process. These results also indicate that pulsed ablative thrusters are relatively inefficient electrothermal devices, as evidenced by the small values of K_I generated. It would be deceptive, however, to draw conclusions regarding optimum geometry for maximum efficiency since there is significant coupling between both Ψ and the geometric configuration of electrode and propellant which have not been considered in this simplified model. For example, in the breech-fed geometry approximately one order of magnitude less mass is generated when compared to the side-fed geometry with identical electrode configuration at the same discharge energy. Equation (7) would imply a thrust efficiency increase of the same order of magnitude, but in fact the value of Ψ in the

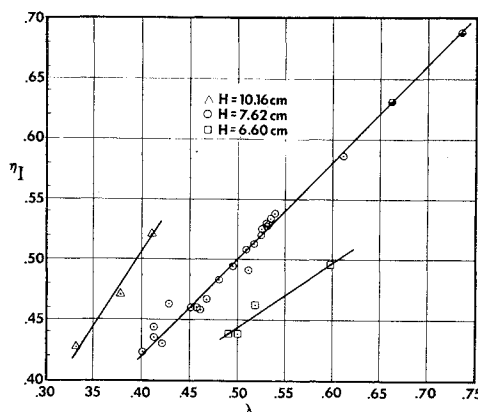


Fig. 7 Impulse bit efficiency as function of λ at three electrode spacings.

breech-fed case is much smaller than that in the side-fed case because the discharge becomes nearly critically damped in the breech-fed case. There is at present no model which would predict this a priori. The dependence of Ψ on geometric factors is evidenced by a correlation between Ψ and $2E/Z$, where Z is the initial circuit plus arc impedance. This correlation is presented in Fig. 8. Note that for $H=10.16$ cm the factor multiplying E/Z is approximately 2.12 and at $H=6.60$ cm the factor is 1.82, with the factor at $H=7.62$ cm falling between these at 1.98. All of the data in Fig. 8 are for the side-fed geometry. Breech-fed data do not fall on this plot. Nevertheless, it can be concluded that minimizing circuit inductance will produce maximum Ψ for a given energy and electrode configuration and, austeriously, maximum efficiency.

The dependence of mass ablated per discharge m on propellant geometry and Ψ is shown in Fig. 9. The geometric factor A_p/A_0 is the ratio of exposed propellant area to surface area open to the vacuum. It is a rough estimate of the fraction of total radiant energy impinging on the propellant surface. It is important to note that increasing Ψ will also increase m for a given electrode/propellant configuration but previous experimentation, wherein Ψ has been increased by increasing E , shows that higher efficiencies are obtained. Thus, the increase in m with Ψ is something less than linear. Moreover, the increase in efficiency obtained by increasing E has been manifested by an increase in I_{sp} at constant thrust/power ratio. It is only changes in the electrode/propellant configuration that have led to changes in T/P . Generally, T/P will increase when a geometric change is introduced which causes ablation of more mass.

This experimentally observed trend is at least qualitatively predicted by Eq. (5) since division by E yields

$$I/E = T/P = K_I (2m/E)^{1/2} + K_2 \Psi/E \quad (8)$$

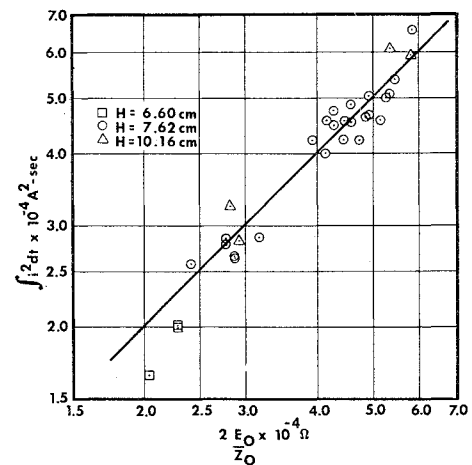


Fig. 8 Dependence of Ψ on $2E_0/Z_0$ for side-fed configuration.

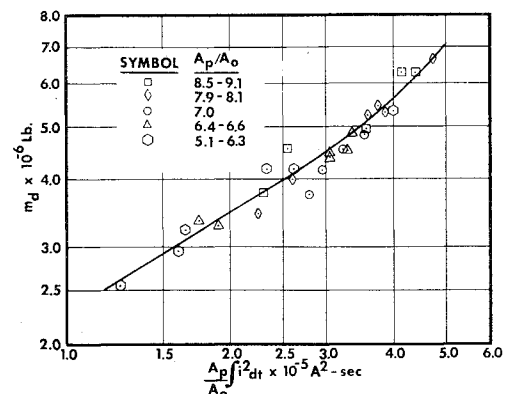


Fig. 9 Dependence of mass ablated per discharge on $(A_p/A_0)\Psi$.

The ratio Ψ/E being fairly constant for a given electrode configuration (cf. Fig. 8), a change in the factor A_p/A_0 at given discharge energy which results in an increase in m will, therefore, increase I/E . This was demonstrated at the 10.16-cm electrode spacing, as mentioned previously. The decrease in thrust efficiency as a result of increasing m with constant electrode configuration and discharge energy is also expected, i.e., from Eq. (7).

It is noteworthy that Eq. (5) was developed without consideration of the effect of included angle between electrodes, yet the data at all angles considered correlate equally well. In addition, it was observed that when the discharge energy was increased from 450 J to 700 J the included angle between electrodes had no effect on performance in the side-fed case. Explanations of these two facts are not available at the present time, but a current program which has the objective of obtaining a more detailed description of the acceleration mechanism in this device will, hopefully, result in explanations of the above anomalies.

Conclusions

The data obtained during this study have shown that pulsed ablative plasma accelerators are capable of a large range in performance as thrusters. Thrust efficiencies up to 53% at a specific impulse of 5160 s were generated using Teflon for propellant. An evaluation of other thermoplastics for use as propellants has shown no performance increase using Celcon, Halar, or Halon, but a 63% increase in specific impulse coupled with an increase in thrust efficiency of 13 percentage points was found using Tefzel. Unfortunately, the decrease in thrust/power ratio from 21.07 to 16.05 mN/kW makes Tefzel less attractive as a propellant. Teflon seeded with 10% and 30% LiOH and InBr produced no increase in performance over Teflon itself.

Introducing an included angle between electrodes has led to increases in both thrust/power and specific impulse of the breech-fed geometry up to 20°. The thrust/power ratio of the side-fed configuration is insensitive to this parameter, but specific impulse is increased as the angle is increased up to 20°. Beyond 20°, a significant decrease in performance was encountered with both geometries. The interelectrode spacing was shown to have a major effect on the form of the discharge, yielding a more oscillatory discharge when decreased at constant initial voltage. This result, coupled with a simple semiempirical analysis, indicates that although larger electromagnetic impulse is produced by a more oscillatory discharge, the relative magnitude of electromagnetic to electrothermal impulse is decreased, leading to a decrease in thrust efficiency.

References

- ¹Guman, W.J. and Nathanson, D.M., "Pulsed Microthruster Propulsion System for Synchronous Orbit Satellite," *Journal of Spacecraft and Rockets*, Vol. 7, April 1970, pp. 409-415.
- ²Vondra, R.J. and Thomassen, K.I., "A Flight-Qualified Pulsed Electric Thruster for Satellite Control," AIAA Paper 73-1067, Lake Tahoe, Nev. 1973.
- ³Palumbo, D.J. and Guman, W.J., "Pulsed Plasma Propulsion Technology," Air Force Rocket Propulsion Lab., Edwards AFB, Calif., Interim Rept. AFRPL-TR-73-79.
- ⁴Palumbo, D.J. and Guman, W.J., "Propellant Side-Feed-Short Pulse Discharge Thruster Studies," Fairchild Republic Co., Farmingdale, N.Y., NASA-CR-112035, Jan. 1972.
- ⁵Stanyukovich, K.P., *Unsteady Motion of Continuous Media*, Pergamon Press, New York, 1960, pp. 147-157.
- ⁶Palumbo, D.J. and Begun, M., "Plasma Acceleration in Pulsed Ablative Arc Discharge," Air Force Office of Scientific Research, Arlington, Va., Interim Rept. AFOSR-75-0618, June 1965.
- ⁷Guman, W.J., "Efficiency Calculations from Thrust Measurements," *ARS Journal*, May 1961, p. 676.

From the AIAA Progress in Astronautics and Aeronautics Series . . .

THERMOPHYSICS AND SPACECRAFT THERMAL CONTROL—v. 35

Edited by Robert C. Hering, University of Iowa

This collection of thirty papers covers some of the most important current problems in thermophysics research and technology, including radiative heat transfer, surface radiation properties, conduction and joint conductance, heat pipes, and thermal control of spacecraft systems.

Radiative transfer papers examine the radiative transport equation, polluted atmospheres, zoning methods, perforated shielding, gas spectra, and thermal modeling. Surface radiation papers report on dielectric coatings, refractive index and scattering, and coatings of still-orbiting spacecraft. These papers also cover high-temperature thermophysical measurements and optical characteristics of coatings.

Conduction studies examine metals and gaskets, joint shapes, materials, contamination effects, and prediction mechanisms.

Heat pipe studies include gas occlusions in pipes, mathematical methods in pipe design, cryogenic pipe design and test, a variable-conductance pipe, a pipe for the space shuttle electronics package, and OAO-C heat pipe performance data. Spacecraft thermal modeling and evaluating covers the Large Space Telescope, a Saturn/Uranus probe, a lunar instrumentation package, and the Mariner spacecraft.

551 pp., 6 x 9, illus. \$14.00 Mem. \$20.00 List

TO ORDER WRITE: Publications Dept., AIAA, 1290 Avenue of the Americas, New York, N. Y. 10019